Performance of a Multifunctional Space Evaporator-Absorber-Radiator (SEAR)

Michael G. Izenson,[1] Weibo Chen,[2] Scott Phillips,[3] Ariane Chepko[4]
Creare, Hanover, NH, 03755

Grant Bue[5]
NASA Lyndon B. Johnson Space Center, Houston, TX, 77058

and

Gregory Quinn[6]
UTC Aerospace Systems, Windsor Locks, CT, 06095

The Space Evaporator-Absorber-Radiator (SEAR) is a nonventing thermal control subsystem that combines a Space Water Membrane Evaporator (SWME) with a Lithium Chloride Absorber Radiator (LCAR). The LCAR is a heat pump radiator that absorbs water vapor produced in the SWME. Because of the very low water vapor pressure at equilibrium with lithium chloride solution, the LCAR can absorb water vapor at a temperature considerably higher than the SWME, enabling heat rejection sufficient for most EVA activities by thermal radiation from a relatively small area radiator. Prior SEAR prototypes used a flexible LCAR that was designed to be installed on the outer surface of a portable life support system (PLSS) backpack. This paper describes a SEAR subsystem that incorporates a very compact LCAR. The compact, multifunctional LCAR is built in the form of thin panels that can also serve as the PLSS structural shell. We designed and assembled a 2 ft² prototype LCAR based on this design and measured its performance in thermal vacuum tests when supplied with water vapor by a SWME. These tests validated our models for SEAR performance and showed that there is enough area available on the PLSS backpack shell to enable rejection of metabolic heat from the LCAR. We used results of these tests to assess future performance potential and suggest approaches for integrating the SEAR system with future space suits.

Nomenclature

A_{LCAR}	is the radiating surface area of the LCAR (m²)
C_f	is the LCAR's final concentration (g LiCl / g solution)
C_0	is the LCAR's initial concentration (g LiCl / g solution)
h_{fg}	is the heat of evaporation of water (roughly 2,500 J/g)

[1] Principal Engineer, P.O. Box 71, Hanover, NH 03755.
[2] Senior Engineer, P.O. Box 71, Hanover, NH 03755.
[3] Engineer, P.O. Box 71, Hanover, NH 03755.
[4] Engineer, P.O. Box 71, Hanover, NH 03755.
[5] Aerospace Technologist, 2101 NASA Parkway, Houston, TX, 77058/Mail Stop EC2.
[6] Staff Research Engineer, UTC Aerospace Systems, 1 Hamilton Road, Windsor Locks, CT 06096-1010/Mail Stop 1A-2-W66.

h_{abs} is the heat of absorption of water in LiCl solution (250–500 J/g, depending on the solution concentration)
$m_{w,a}$ is the mass of water absorbed (kg)
m_{LiCl} is the mass of LiCl in the LCAR (kg)
q is the rate of heat rejection by thermal radiation (W)
T_{LCAR} is the surface temperature of the LCAR (K)
T_{env} is the temperature of the environment seen by the LCAR (K)
ε is the emissivity of the LCAR radiating surface (--)
σ is the Stefan-Boltzmann constant (5.67×10^{-8} W/m^2-K^4)

I. Introduction

Heat rejection from space suits is a critical life support function that presents significant engineering challenges. Space suits are heavily insulated to protect spacewalking astronauts from extreme thermal environments; however, this insulation traps metabolic heat inside the suit. Current technology uses a circulating water loop to absorb heat inside the pressure garment, then transport the heat to a block of water ice in a sublimator. The ice in the sublimator absorbs heat from the circulating water by gradually vaporizing and venting steam into the surrounding vacuum. This system has an extensive flight heritage (dating back to the Apollo program) but consumes about 8 lb_m (3.6 kg) of water for a typical EVA sortie. Recently NASA has developed a Space Water Membrane Evaporator (SWME) to replace the sublimator with a device that has better long-term performance characteristics. The SWME evaporates circulating water directly from a bundle of porous, hydrophobic hollow fibers. Expendable cooling with a sublimator or SWME is highly practical for operations in low-Earth orbit where resupply is relatively simple. However, cooling by consuming water would place severe constraints on EVA for future exploration missions that call for extended operations at great distances from Earth. A prior paper presented data showing the very large impact of conventional spacesuit cooling on ECLSS mass for future exploration missions (Bue et al. 2013). For long missions (575 days), water consumed during EVAs can amount to 2,500 kg, or over 30% of the total ECLSS mass.

This paper describes recent advances in the Space Evaporator-Absorber-Radiator (SEAR) technology. The objective of a SEAR is to dramatically reduce the use of consumables for EVA thermal management. SEAR combines the SWME with a Lithium-Chloride Absorber Radiator (LCAR) that rejects heat mainly by thermal radiation from a compact, high-temperature radiator. Figure 1 shows how the SEAR system is related to conventional thermal control technology. Figure 1a illustrates conventional technology, in which a SWME rejects heat from the life support system by venting water vapor to space. Both the SWME and the liquid cooling garment (LCG) operate at a temperature of about 20°C, with variations due to the astronaut's metabolic rate. Figure 1b shows a SEAR system, in which water vapor is absorbed in an LCAR instead. The LCAR uses a batch process, regenerable, absorption heat pump to capture water vapor produced in the SWME. LiCl/water solution in the LCAR is a powerful desiccant that maintains a very low vapor pressure even at relatively high temperatures. Water vapor from the SWME condenses and is absorbed in the solution. The heat generated in this process radiates to space from the surface of the LCAR. Since the vapor pressure over the solution is so low, this process can occur at temperatures that are typically 30°C higher than the SWME temperature. This enables the LCAR to operate as a heat pump, rejecting heat at temperatures of about 50°C which significantly reduces the size of the radiator.

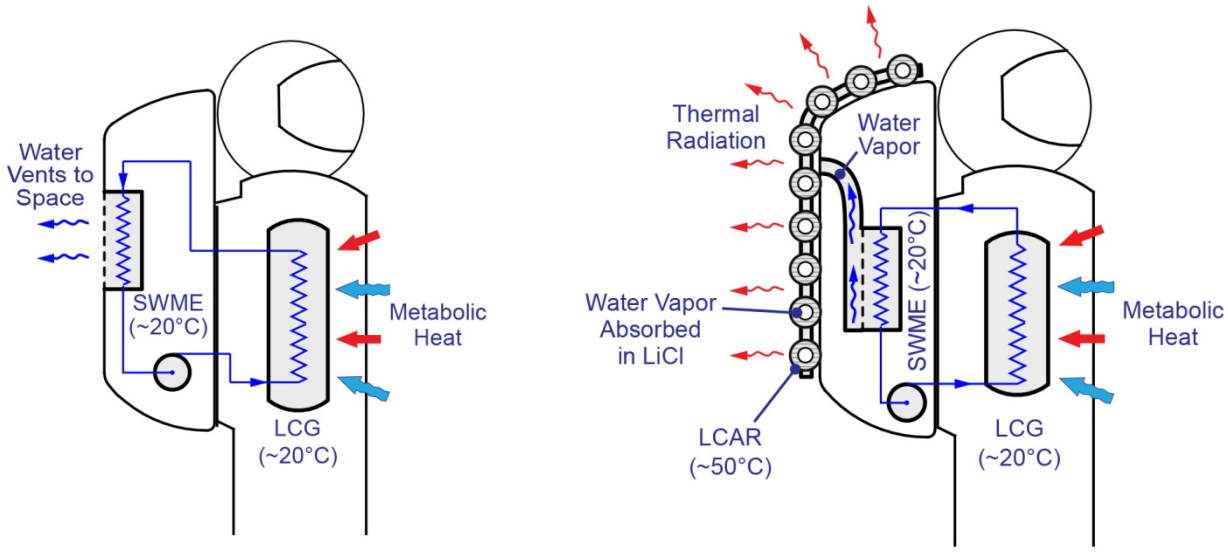

(a) Heat rejection using SWME **(b) Heat rejection using SEAR with flexible LCAR**

Figure 1. Evolution of early SEAR concept.

Since any noncondensible gas in the cooling water will evolve in the SWME and flow to the LCAR, efficient management of noncondensible gas in the LCAR is an important design requirement. Noncondensible gas in the LCAR will behave like noncondensibles in variable-conductance heat pipes. The gas will flow with water vapor until the water vapor condenses, leading to gradual accumulation of the gas at stagnation points in the flow field. LCARs are therefore designed with vents to remove the noncondensibles. These vents can be used either intermittently or continuously. In an intermittently vented system, the LCAR is vented to space periodically to eliminate the noncondensibles from the internal volume. In a continuously vented system, an appropriately sized capillary tube connects the "far end" of the LCAR (where noncondensibles accumulate away from the water vapor inlet) to external vacuum for continuous bleeding. Both approaches result in the loss of a small amount of water, but in either case the amount of water lost is orders of magnitude smaller than the amount of water vapor lost from systems that provide cooling by venting water vapor.

Figure 2 and Figure 3 show current embodiments of the SWME and LCAR technology. Figure 2 is a photograph of the Gen 1 SWME, which uses a 16 cm-long bundle of 14,900 hollow fibers in parallel to evaporate water into the shell-side vacuum space. The Gen 1 SWME has been tested extensively and has been found to meet system requirements for space suit thermal control (Bue et al. 2010). Figure 3 is a photograph of the flexible LCAR prototype that was used in the first SEAR demonstration. The LCAR is a compact heat/mass exchanger that comprises an array of LiCl absorber elements in good thermal contact with the radiating surface and with an array of flow passages for water vapor that enables efficient operation during both absorption and regeneration. The absorber elements are precision-cut sponge elements that contain the liquid LiCl solution by capillary forces. At very high concentrations, the solution is solid and remains in the pores of the sponges. Prior papers (Izenson et al. 2008; Izenson and Chen et al. 2009) provide a detailed description of the flexible LCAR. The Gen 1 SWME and flexible LCAR were coupled to create the first SEAR system and tested under thermal vacuum conditions in Chamber N at NASA JSC in 2012 (Bue et al. 2013). These tests were highly successful, and demonstrated the feasibility of nonventing thermal control using a SEAR system. They also pointed the way toward improvements in the LCAR design that would make the SEAR system more attractive for future programs.

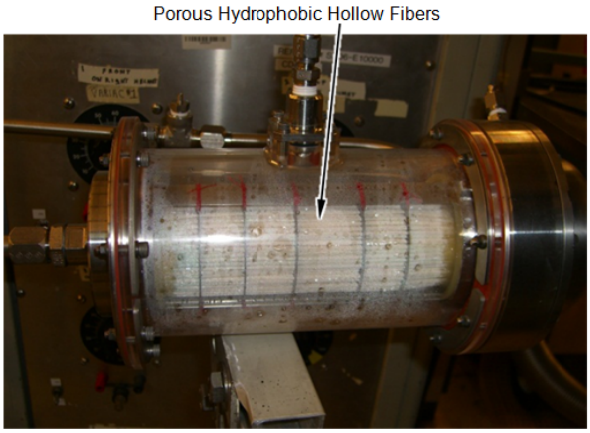

Figure 2. NASA's Space Water Membrane Evaporator (SWME).

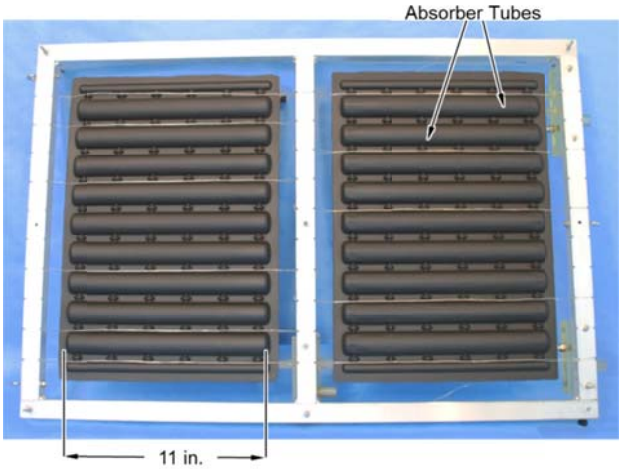

Figure 3. Flexible LiCl Absorber/Radiator (LCAR) Modules.

This paper describes an improved SEAR with a multifunctional structure that builds on lessons learned from the 2012 tests. The new design has the following objectives:

- Minimal impact on PLSS volume using a new, multifunctional honeycomb structure to house the absorber/radiator.
- A multifunctional design that provides both heat rejection and an outer shell for the PLSS backpack.
- Incorporation of lessons learned from 2012 tests. In particular, an improved internal structure that provides much more uniform panel temperatures for thermal radiation and prevents freezing of water vapor in parts of the panels that are exposed directly to low temperature.

Figure 4 shows the basic concept for the multifunctional SEAR with a honeycomb LCAR. Absorber elements are installed in the honeycomb cells of thin, flat panels that double as the structural shell for the PLSS backpack. The honeycomb cells are built with features that allow water vapor and noncondensible gas to flow freely through the panel structure.

Figure 5 shows the concept for each honeycomb cell. Each cell contains LiCl absorber elements and highly conductive graphite elements to couple the absorbers to the LCAR's radiating surface. The honeycomb contains features that enable water vapor to flow to or from each of the cells.

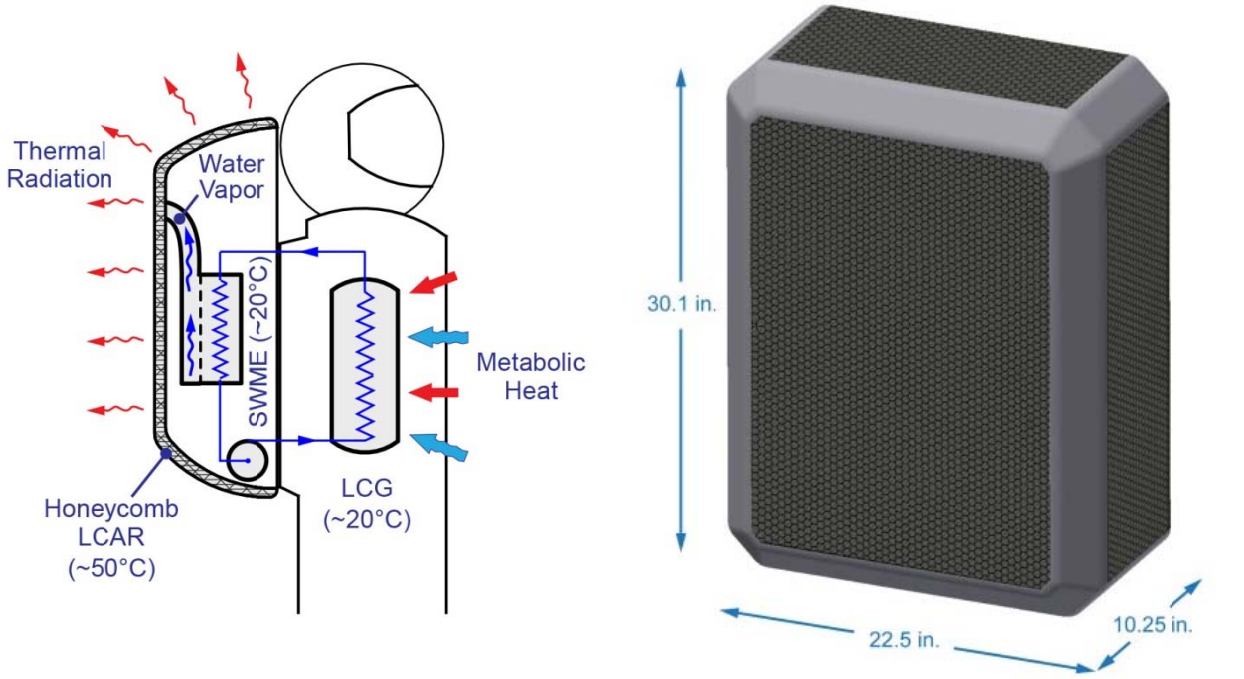

(a) SEAR with multifunctional LCAR

(b) The structural shell for the PLSS can be assembled from five honeycomb LCAR panels

Figure 4. Concept for the multifunctional SEAR.

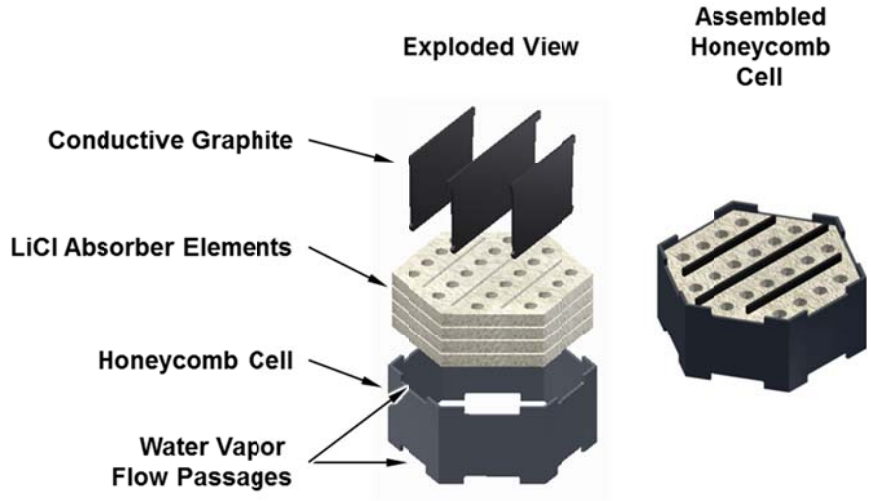

Figure 5. Concept for honeycomb cell structure.

II. Honeycomb LCAR Functional Demonstrator

Production of a honeycomb LCAR like the one described in Section I will require a significant effort to develop the fabrication technology needed to minimize overall mass. Before making that effort, we undertook a demonstration and testing program to prove that the honeycomb design concept will meet thermal performance goals. We built a simplified prototype that incorporates the key thermal/fluid characteristics of the honeycomb panel

in a design that is simpler to build and test. Figure 6 and Figure 7 show the basic concept for this functional demonstrator, in which the honeycomb structure is replaced with machined panels that provide an array of cavities that accommodate absorber elements. Although the packing fraction of absorber elements in the prototype is not as high as could be achieved in a true honeycomb panel, the machined design will have many similar fabrication challenges and its thermal/fluid performance should approximate a true honeycomb panel. The prototype is built up from a stack of thin, machined laminations. Figure 7 shows a cross section through an absorber cavity in the prototype. The two lattice layers provide flow paths for water vapor and noncondensible gas.

The basic design parameters for the LCAR panel were specified based on first-order analysis of the dominant heat, mass, and momentum transfer processes that govern operation as well as first-order structural analysis and experience with prior LCAR systems.

- We specified the dimensions of internal vapor flow passages and the capillary vent tube based on analysis of pressure losses due to vapor and noncondensible gas flow under conditions of maximum heat transfer.
- We specified the radiating area and internal heat conduction paths based on an analysis of external radiation heat transfer and conduction heat transfer through the structure under conditions of maximum heat transfer.
- We specified structural design parameters based on first-order analysis of stresses due to internal and external pressure in the most extreme operating environments.
- We specified the dimensions and maximum LiCl loading of the absorber sponges based on experience with prior generation LCARs.

A detailed analysis of LCAR performance that accounts for all internal heat, mass, and momentum transfer processes as a function of time and position within the panel is a very complex problem which we have not yet undertaken. This type of analysis is recommended for future work when the LCAR would need to be optimized for a specific mission.

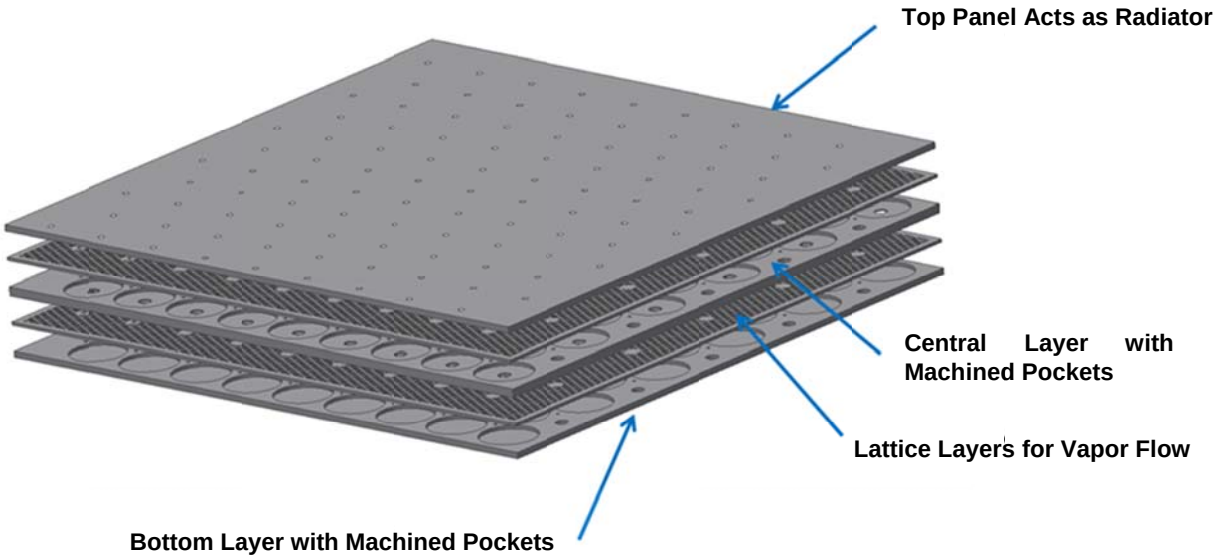

Figure 6. Process demonstrator, flat panel LCAR.

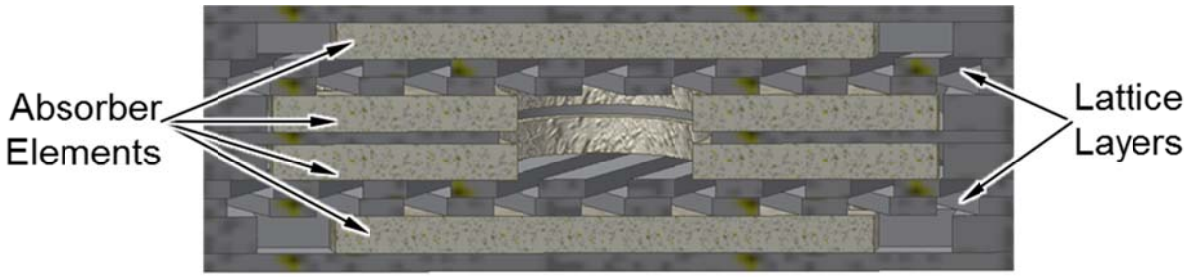

Figure 7. Internal structure of the prototype LCAR.

The structural elements of the process demonstrator were machined from thin sheets of high-conductivity graphite. Figure 8 is a photograph of the process demonstrator during assembly, showing one of the lattice layers in place over the central panel holding an array of absorber sponges. Figure 9 shows two views of an assembled LCAR panel after attaching manifolds, fittings, and instrumentation. Figure 9a shows the radiating side, which faces a cooled shroud during testing and corresponds to the outboard face of the LCAR in the PLSS shell assembly shown in Figure 4. Figure 9b shows the opposite side of the LCAR, which is insulated in our tests and corresponds to the inboard faces of the LCAR panels shown in Figure 4. During testing, one of the fittings is coupled to the SWME (or equivalent vapor source) while the other fitting is coupled to a vacuum pump for periodic venting or continuous venting through a capillary tube. An array of thermocouples attached to the radiating surface measures temperature uniformity.

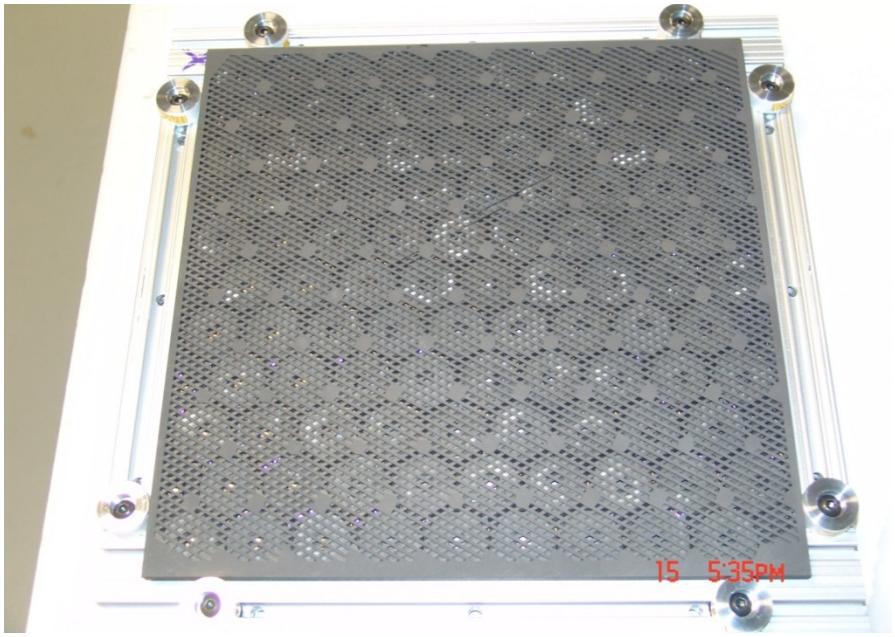

Figure 8. Flow lattice and central panel after bonding.

(a) Radiating side

(b) "PLSS-facing" side

Figure 9. LCAR panel with vapor fittings and thermocouples attached.

III. Thermal Vacuum Test Facility

We built and calibrated a thermal vacuum test facility to measure the performance of the flat panel LCARs. The facility simulates space by providing a thermal environment in which radiation heat transfer dominates, and provides well-controlled boundary conditions that enable a confident assessment of thermal performance.

A. Test Facility Design

The facility comprises a vacuum bell jar with an internal test assembly that supports the LCAR panels between a pair of cryogenically cooled shrouds. The photographs in Figure 10 show the vacuum bell jar and the internal frame assembly that supports the LCARs and shrouds. The right-hand photo shows the back sides of one of the cryogenically-cooled shroud panels. The chamber can accommodate two 12 in. square LCAR panels in a back-to-back, stacked configuration, each facing a 14 in. square cooling shroud. At a separation distance of 0.5 in., this geometry provides a view factor of 0.98 from the radiating side of each LCAR panel to the corresponding shroud, ensuring that we are able to accurately control and measure the heat transfer from the radiator panels. We coat the radiating surfaces of the LCAR panels and the shrouds with LORD Corporation Aeroglaze Z306 coating. Aeroglaze is low-offgassing for good vacuum performance and provides a high emissivity surface ($\varepsilon = 0.9$) for efficient radiation heat transfer.

The vacuum chamber could maintain vacuum levels in the range from 10^{-5} to 10^{-6} torr. At this level of vacuum, the thermal conductivity of the remaining gas in the system will be less than 2×10^{-5} W/m-K, effectively preventing heat conduction from the LCAR panels to the shroud. For example, for an LCAR temperature of 323 K and a shroud temperature of 180 K, the calculated radiation heat transfer will be roughly 46 W compared to a calculated conduction heat transfer of less than 2 mW.

The schematic in Figure 11 shows the overall test setup. Water vapor is generated in an external loop by either the SWME or a custom capillary evaporator built by Creare. Heat to generate the water vapor is provided by a circulating water loop that is maintained at a constant temperature of roughly 20°C using a laboratory chiller. Platinum Resistance Thermometers (PRTs) at the inlet and outlet of the evaporator along with a calibrated rotameter provide calorimetric data to measure the amount of heat transfer from the circulating loop that produces water vapor. Water vapor flows into the vacuum bell jar and then into the pair of LCAR panels. The far ends of the panels are plumbed together, so that noncondensible gas from the panels flows through a capillary tube, then through a desiccant bed, and finally to a vacuum pump that exhausts to ambient.

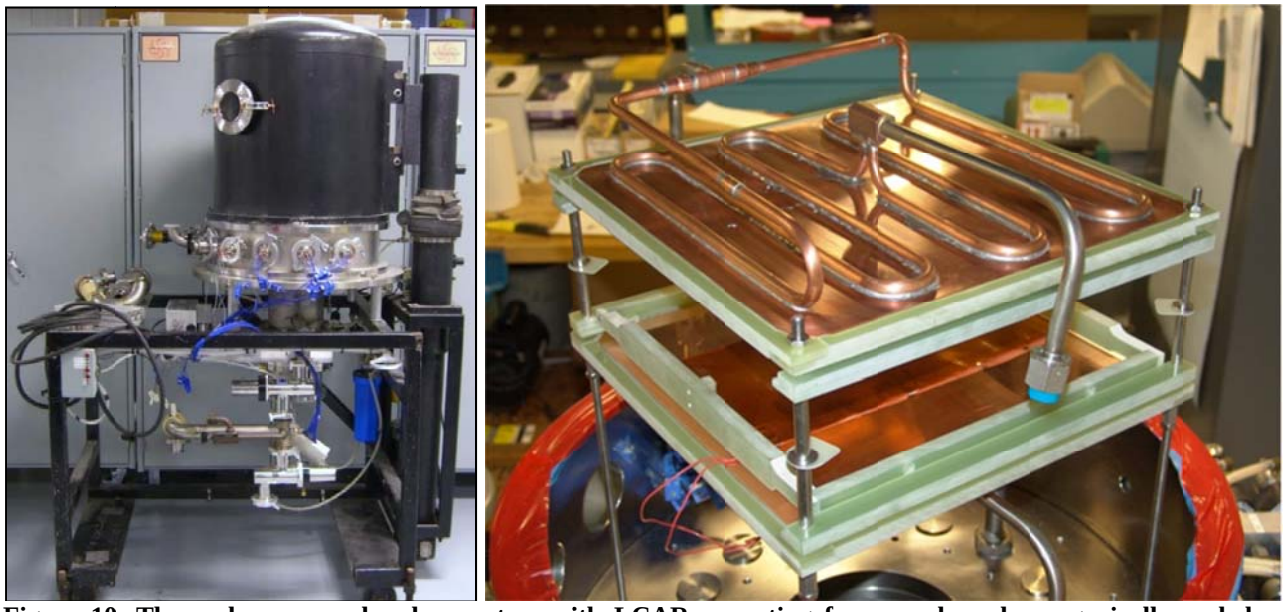

Figure 10. Thermal vacuum chamber system with LCAR mounting framework and cryogenically-cooled panels.

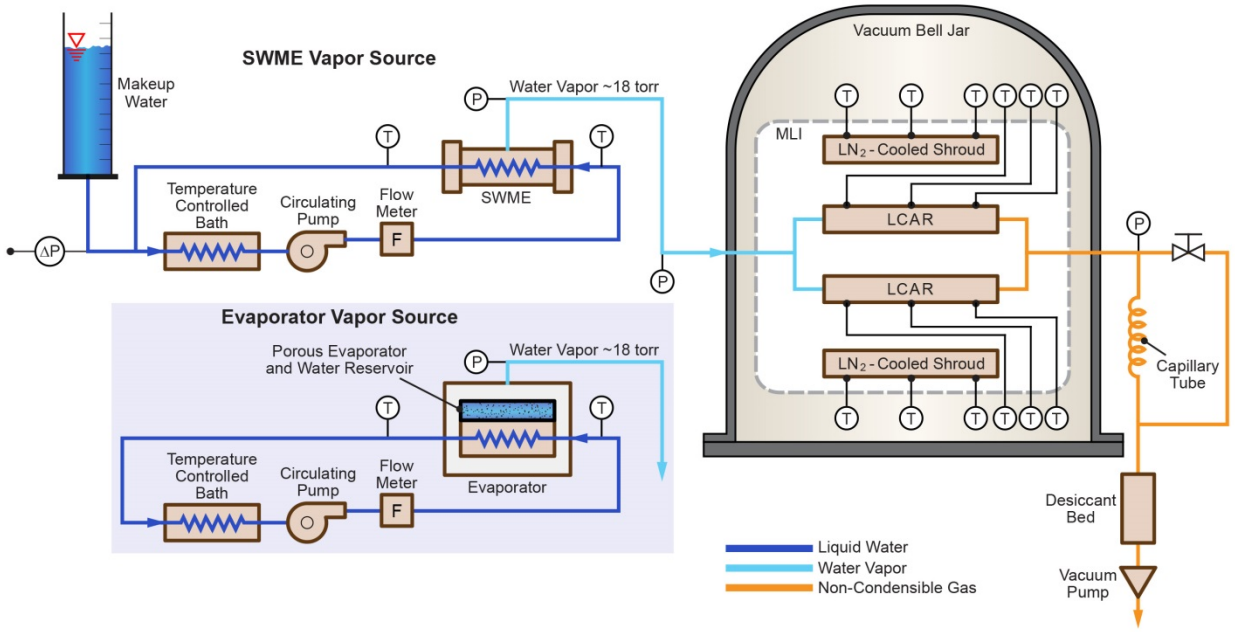

Figure 11. SEAR test facility.

Multi-layer insulation (MLI) between the two LCAR panels (facing each panel's non-radiating side) limits the heat transfer between the panels. We also surround the entire shroud assembly with MLI to insulate the test hardware from the room-temperature walls of the bell jar. Each LCAR panel is supported by four small-diameter stainless steel pins that are held in place by G10 phenolic frames mounted on four posts. The very low thermal conductance of the stainless steel pins (roughly 0.12 mW/°C for each pin) insulates the panels from the frames. These mounting frames allow us to easily remove the LCAR panels after each test and weigh them to measure the quantity of water absorbed.

B. Test Matrix and Measurements

Table 1 summarizes the test matrix, which began with a thermal calibration test (using an electrically-heated radiator) and went on to include tests using one and two flat panel LCARs and two sources of water vapor. Shroud temperatures were set at 180 and/or 250 K, to simulate cold and 1-sun thermal radiation environments. Water vapor was supplied either from the SWME or from a Creare evaporator developed to support LCAR testing. The steady state performance of the Creare evaporator and the SWME were very similar, so most of the tests were run with the Creare evaporator to simplify testing. Tests with the SWME were used mainly to confirm similar performance.

Between tests, the LCARs were regenerated by heating to 120°C for 4 hours while under vacuum (0.5 to 2.0 torr, corresponding to the vapor pressure of water in the system). At the end of this process, the LiCl concentration in the absorber sponges exceeds 90%. The system is able to operate with these high concentrations—corresponding to crystallized LiCl—because the solution does not flow during operation of the LCAR. This method for regenerating the LCAR is similar to methods that could be used on future space exploration missions. In a manned spacecraft module or habitat, water exhausted from the vacuum pump would enter the internal atmosphere and be recovered by a condensing heat exchanger or other water recovery equipment in future environmental control and life support systems.

Table 2 lists the key instrumentation used during testing. LCAR temperatures were measured with an array of thermocouples attached to the radiating and insulated surfaces. We attached multiple TCs to the radiating surface of each LCAR panel to provide measurements of temperature uniformity. An additional TC was attached to the back, insulated side of each panel to measure the average, internal temperature. Water vapor pressures were measured in both the evaporator and LCAR. The saturation pressure in the evaporator is a measure of the average cooling temperature provided by the SEAR system. Power input to the evaporator was calculated by calorimetry on the water that flowed through the SWME or the heat exchanger in the evaporator. Finally, the water absorbed in each test was measured by weighing the LCAR panels (uncoupled from the rest of the system) before and after each absorption and regeneration.

Table 1. Test matrix.			
	Shroud Temperature (K)	Water Vapor Source	Venting
Thermal calibration	180, 250	—	—
Single panel	180, 235	Creare evaporator	Intermittent
Dual panel SEAR	180, 250	SWME, Creare evaporator	Intermittent
Dual panel	180, 250	Creare evaporator	Continuous

Table 2. Instrumentation.			
	Instruments	Locations	Accuracy
LCAR surface temperature	Type T Thermocouples	Nine locations across each LCAR radiating surface	±1.0°C
LCAR back temperature	Type T Thermocouples	Center of each insulated LCAR surface	±1.0°C
SWME or evaporator pressure	Kurt Lesker diaphragm vacuum gage	At SWME or evaporator outlet	±1.0 torr
LCAR pressure	Kurt Lesker diaphragm vacuum gage	At water vapor inlet to vacuum chamber, ~24 in. of tubing upstream from LCAR	±1.0 torr
SWME or evaporator power	Calibrated PRTs and calibrated rotameter	Circulating water inlet and exit from SWME or evaporator	±5 W
Water absorption	Scale	—	±0.5 g

C. Thermal Calibration

Before installing LCAR panels, we installed two "dummy" radiators made from copper panels instrumented with thermocouples and attached to thin-film resistance heaters. We installed six thermocouples on the radiating surfaces of each radiator and shroud to measure the temperature distribution. Figure 12 shows the average of temperatures recorded from the upper and lower radiators and shroud panels during thermal calibration testing. During this test, we controlled both the heat input to the radiator and the temperature of the shroud. There were four test points: 15 W / 250 K, 30 W / 250 K, 30 W / 180 K, and 50 W / 180 K. Key data were the radiator temperature and the uniformity of the shroud temperature. The radiator temperatures are quite uniform for both the lower and upper radiators, and are consistent with the results of radiation heat transfer calculations assuming an Aeroglaze emissivity of 0.90. The upper shroud temperatures were also quite uniform at 250 K (±2.5 K, corresponding to a heat flux variation of ±2.5%) and slightly less uniform at 180 K (±15 K, corresponding to a heat flux variation of ±4%). The lower shroud had slightly greater temperature variation at the 250 K test point (±5 K, corresponding to a heat flux variation of ±5%) and roughly similar variation for the 180 K test point.

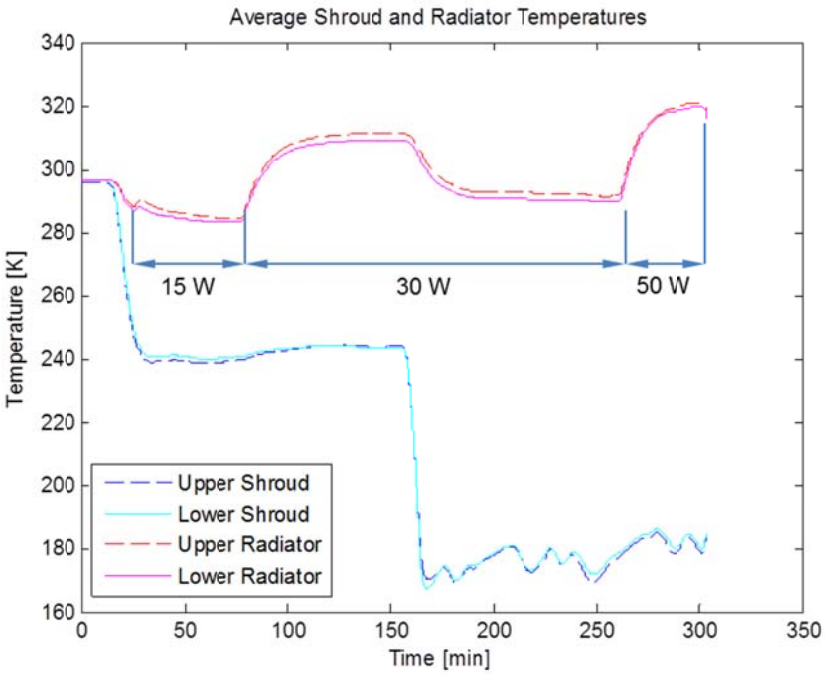

Figure 12. Average radiator and shroud temperatures in tests using the dummy radiator.

IV. LCAR Performance

We measured performance of the functional demonstrator in a series of three tests that differ in the number of LCAR panels and the method of venting noncondensibles. They are: (1) a test using a single LCAR with intermittent venting, (2) dual LCARs with intermittent venting, and (3) dual LCARs with continuous venting through a capillary tube.

Test of Single LCAR Panel. The first test of a flat panel LCAR used a single panel only with vapor supplied by Creare's evaporator. The test shows that the flat panel design achieves its goal of a much more uniform surface temperature than the earlier flexible LCAR design. Figure 13(a) shows temperatures recorded from the radiating surface. At the beginning of this test, the LCAR was isolated and was cooling due to radiation to the shrouds. At t≈20 min, the valve between the LCAR and the evaporator was opened, allowing water vapor to enter the LCAR. Condensation and absorption in the LiCl solution caused the LCAR temperature to increase rapidly to the range 120 to 140°F (49 to 60°C). The process proceeded continuously (with occasional venting of noncondensible gas) for about 200 minutes. During this time, the radiator temperature decreased gradually as the LiCl solution became more dilute. The valve was closed at t≈220 min, resulting in rapid cooling of the LCAR as condensation and absorption ceased.

For comparison, Figure 13(b) shows temperatures measured in 2012 from the surface of the second-generation LCAR during tests in Chamber N at NASA JSC. Comparison of these plots shows that the honeycomb LCAR design produces a much more uniform temperature on the radiating surface. Surface temperature uniformity of the honeycomb LCAR was approximately ±10°F (±5.6°C) during absorption while the variations in the second-generation LCAR were ±60°F (±33°C). Furthermore, the high thermal conductivity of the graphite structure combined with the highly parallel flow structure for water vapor has eliminated problems of local condensation and freezing. For the honeycomb unit, all the measured surface temperatures remained well above freezing throughout the entire test. The second-generation LCAR showed some freezing early in testing (t≈80–90 min) and an extended period later in the test (t≈25–400 min).

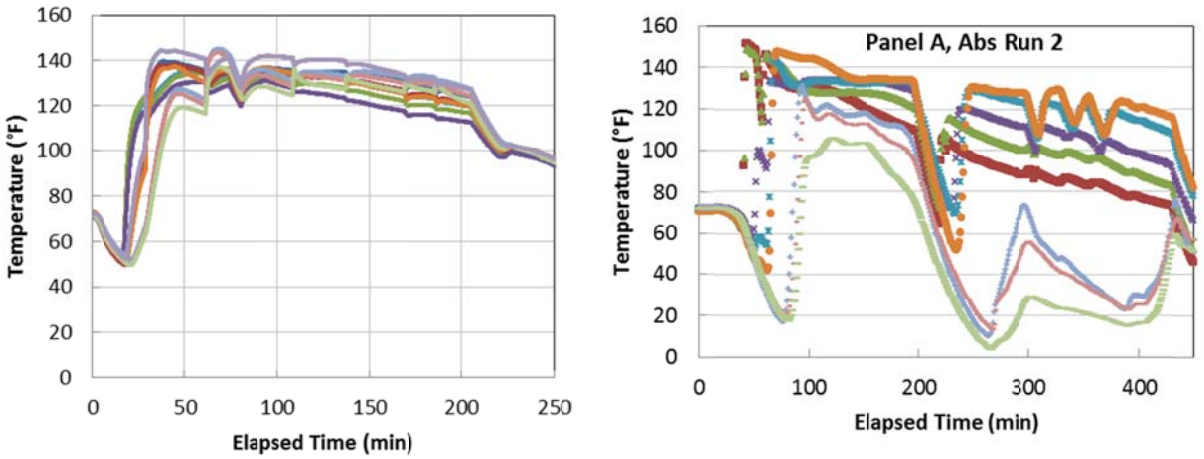

(a) Honeycomb LCAR **(b) Flexible LCAR**

Figure 13. Honeycomb LCAR surface temperatures (a) during absorption/radiation are much more uniform than the flexible LCAR (b) (data from test of single LCAR panel).

Dual Panel Tests. We ran two tests using dual LCAR panels. The first test (on 12/18/13) used both the SWME and the Creare evaporator as sources of water vapor for tests at two different shroud temperatures (173 K and 248 K) with periodic venting used to eliminate noncondensible gas. Table 3 lists the shroud and LCAR temperatures for each test point as well as thermal power deduced from thermal radiation calculations and from calorimetry on the water vapor source. To characterize the LCAR temperatures for thermal radiation calculations, we used the temperatures measured by thermocouples that were attached to the back side of each panel—that is, the side facing the other LCAR panel. We found that the thermocouples attached to the front side read low due to conduction from the junction down the thermocouple lead, which was cooled by radiation. The difference in computed radiation powers is 4 to 5 W. The water supply power is computed by calorimetry. We believe that the calorimetry value is more accurate for the SWME because of the reduced thermal mass of the fiber bundle compared to the metal evaporator structure. Radiated powers are higher than the SWME power, which is expected due to the additional heat of absorption that must be radiated.

Table 3. Thermal power calculations for first dual LCAR test (12/18/13).

Water Vapor Source	SWME	SWME	Evap	Evap
Approximate Shroud Temperature (K)	173	248	173	248
Upper LCAR Back Temperature (°C)	33.3	43.7	35.6	45.6
Lower LCAR Back Temperature (°C)	45.6	47.3	46.2	50.4
Powers:				
Upper Q rad-shroud (diffuse-grey) (W)	35.1	27.9	36.1	28.4
Lower Q rad-shroud (diffuse-grey) (W)	40.5	29.4	41.5	30.6
Total Radiation Power (W)	75.6	57.4	77.6	59.0
Water Supply Power (W)	65.5	60.2	97.8	52.5

Figure 14 plots the LCAR back temperatures, and Figure 15 and Figure 16 plot the temperatures measured by individual thermocouples on the radiating and shroud surfaces for the lower and upper LCAR/shroud assemblies, respectively. Data recorded early in this test show the temperatures as we adjusted the shroud cooling system to achieve the desired test conditions by controlling liquid nitrogen flow rates and heater powers. To maintain the LCAR temperatures during this period above freezing, we initiated a small flow of water vapor from the evaporator at $t \approx 40$ min. At $t \approx 60$ min conditions had stabilized at the desired levels and we began recording data for the planned test points. The temperature fluctuations during this period are due to periodic venting of noncondensible gas from the LCAR. Figure 14 (and the summary data points in Table 3) shows that the lower LCAR was operating at a slightly warmer temperature than the upper LCAR. We believe that this is probably due to differences in vapor

flow between the two panels, indicating that future work should address the need to ensure uniform vapor flow to multiple LCAR panels operating in parallel. The difference in LCAR panel temperatures cannot be due to the difference in shroud temperature, because in both cases the shroud temperature is much less than the LCAR temperature. The radiative heat flux, which is proportional to $T_{LCAR}^4 - T_{shroud}^4$, is almost independent of the shroud temperature under these conditions. The individual TC data for each LCAR in these tests (Figure 15 and Figure 16) are similar to the data for the single panel test, indicating good uniformity and no instances of flow blockage leading to excessive cooling. The LCAR surface temperatures also tend to be grouped in threes, corresponding to the 3×3 layout of the thermocouples on the radiating surface. Each group of three similar temperatures corresponds to a set of TCs located the same distance between the inlet and exit manifolds.

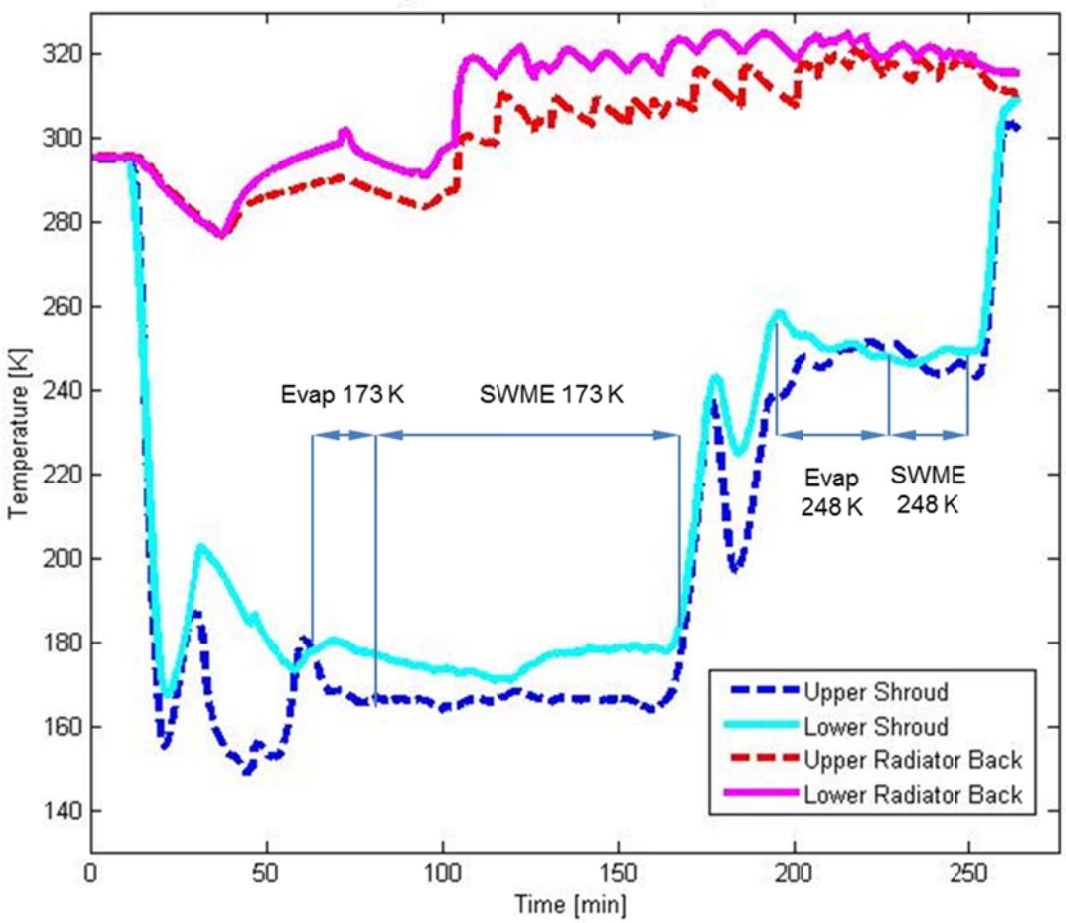

Figure 14. LCAR back and average shroud temperatures (12/18/13).

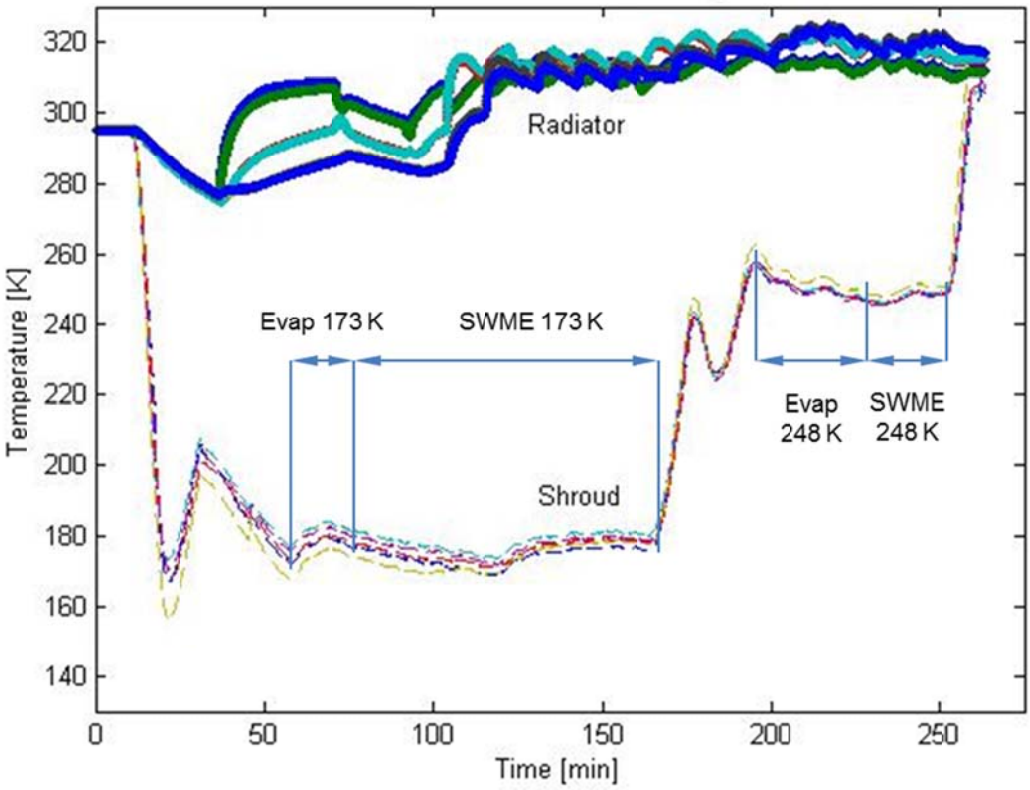

Figure 15. Lower LCAR and shroud temperatures (12/18/13).

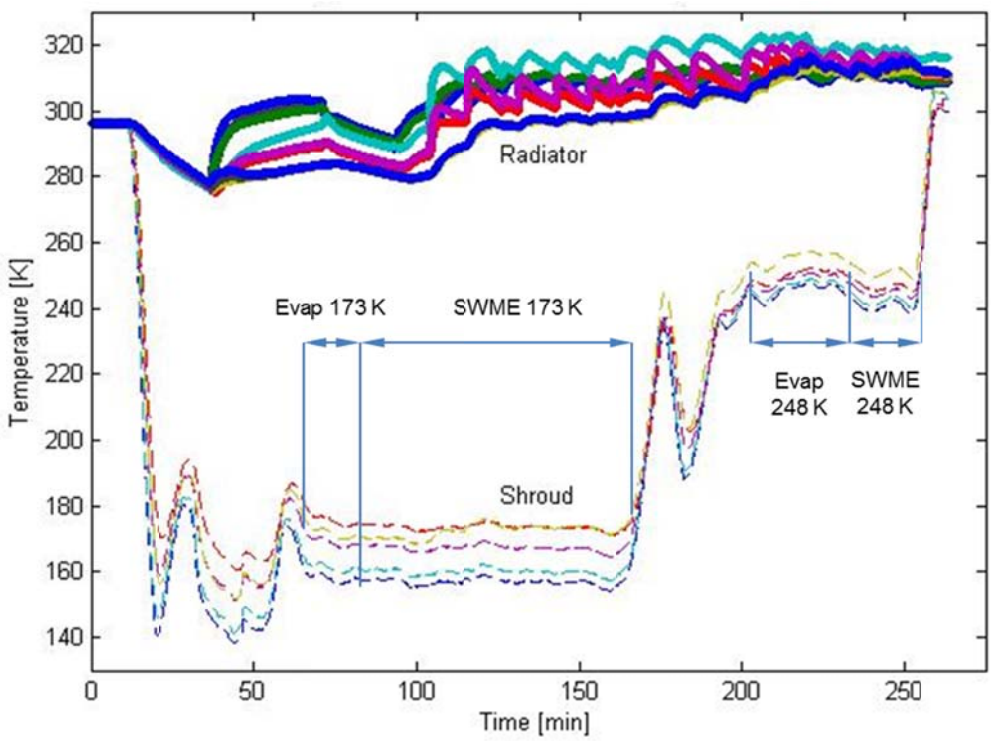

Figure 16. Upper LCAR and shroud temperatures (12/18/13).

Figure 17 plots the temperature differences measured in the circulating loops that heated the SWME and the Creare evaporator. Temperature differences during operation were generally 3 to 4°C. Note that the SWME responds much more rapidly when activated due to the lower thermal mass of the fiber bundle compared to the Creare evaporator. The periodic temperature fluctuations observed in the LCAR panel correspond with the pressure variations due to periodic venting of noncondensible gas.

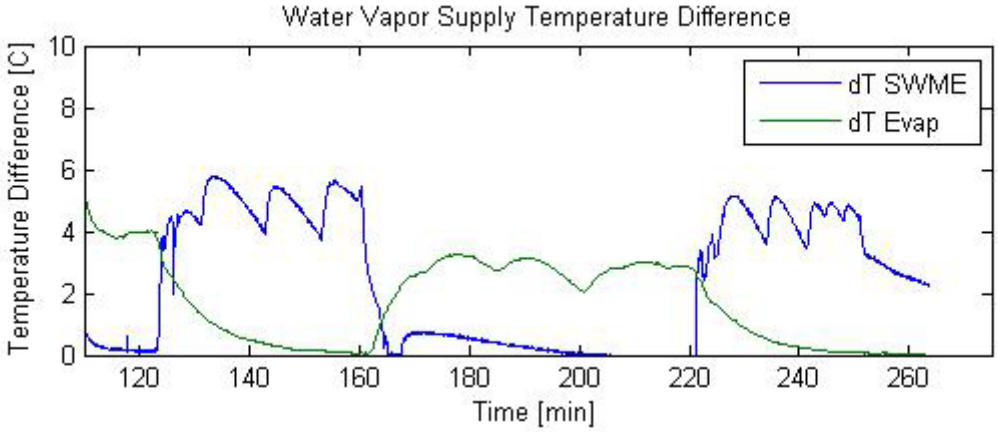

Figure 17. Temperature difference across SWME and evaporator (12/18/13).

A second test of dual LCAR panels was run on 1/8/14. This test used only the Creare evaporator as a heat source, vented noncondensible gases continuously through a capillary tube,[7] and shows the effects of gradually closing the control valve between the evaporator and the LCAR pair. Table 4 lists the shroud and LCAR back temperatures for each operating point. As the valve was closed, vapor pressure in the LCAR panels decreased, resulting in lower radiating temperatures and lower rates of heat transfer. The thermal power estimated by calorimetry varies by a factor of three between fully open and mostly closed. We believe the variation in power in this test is indicated better by the calorimetry loop, since the thermal mass of the radiator slowed its adjustment to new power levels while the evaporator temperature adjusted more quickly.

Table 4. Thermal power calculations for second dual LCAR test (12/18/13).

Control Valve Position		Fully Open	Partially Closed	Mostly Closed	Fully Open
Average Upper Shroud Temperature	(K)	175.6	176.7	174.4	173.5
Average Lower Shroud Temperature	(K)	173.6	174.2	172.2	173.1
Upper LCAR Back Temperature	(°C)	41.7	41.0	19.2	27.7
Lower LCAR Back Temperature	(°C)	50.0	44.2	23.1	33.5
Water Supply Power	(W)	88.9	69.7	31.6	77.4

Figure 18 and Figure 19 show the LCAR and shroud temperatures measured during this test. Overall behavior is similar to the first test with dual LCARs, except that with continuous venting there were no periodic temperature fluctuations. Figure 20 plots the temperature drop in the circulating water after flowing through the evaporator.

[7] Capillary tube dimensions are 9.25 in. long, 0.125 in. outer diameter, 0.069 in. inner diameter.

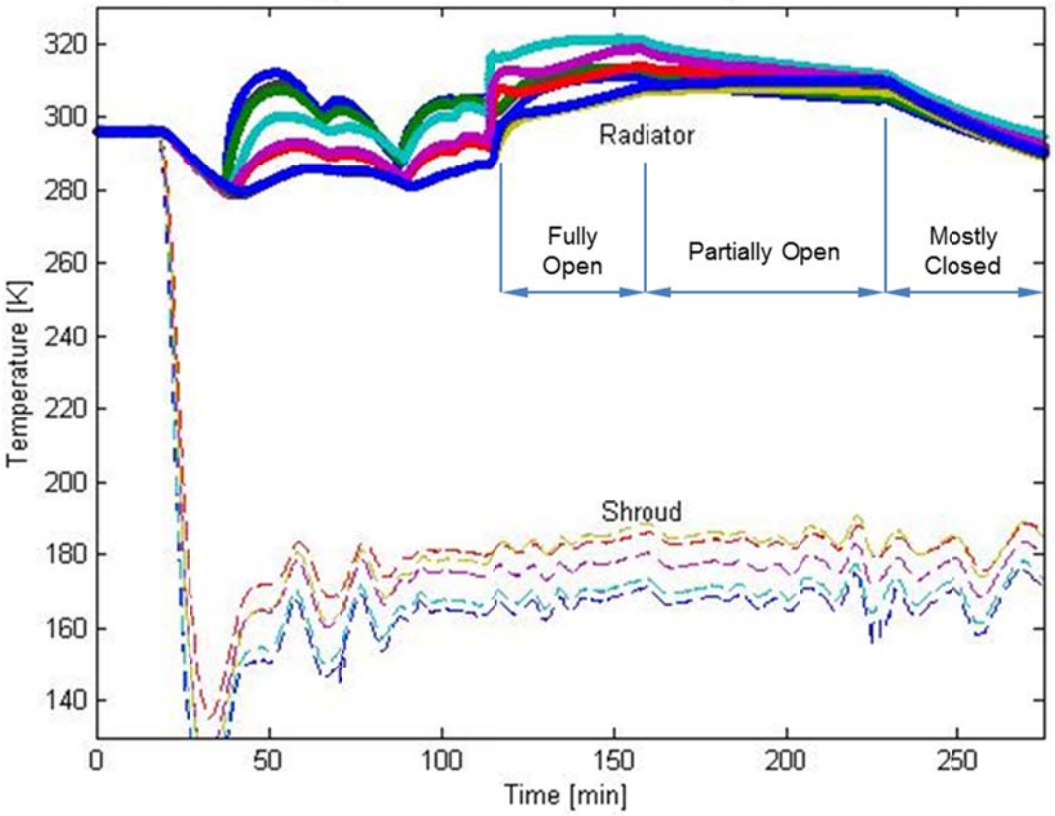

Figure 18. Upper LCAR and shroud temperatures (1/8/14).

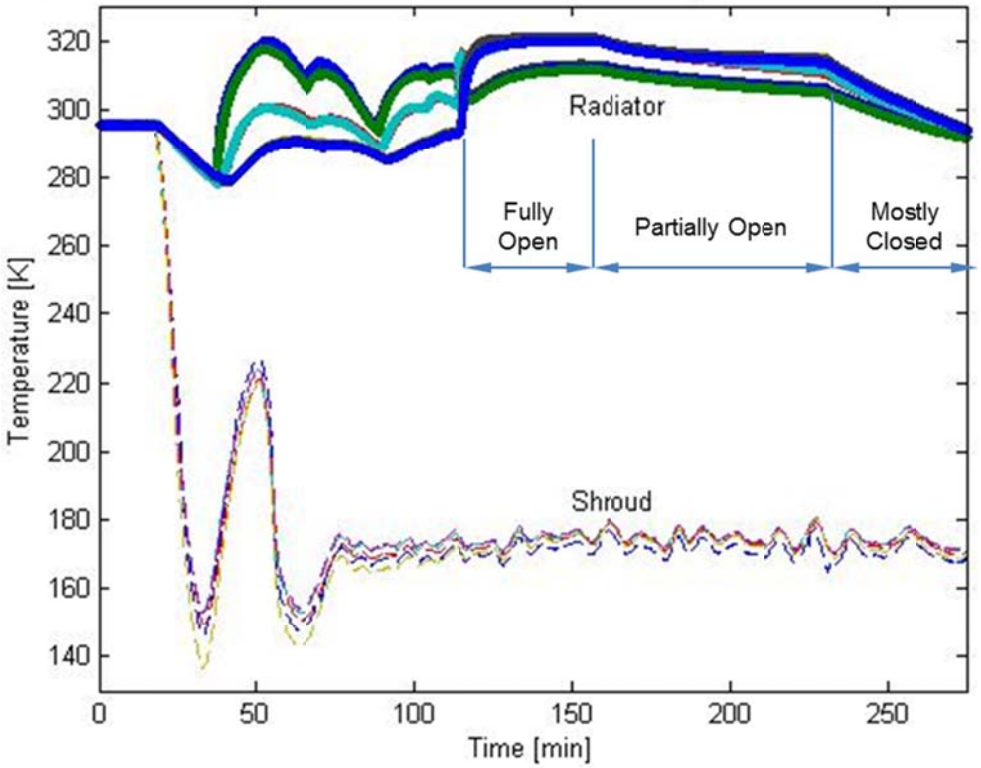

Figure 19. Lower LCAR and shroud temperatures (1/8/14).

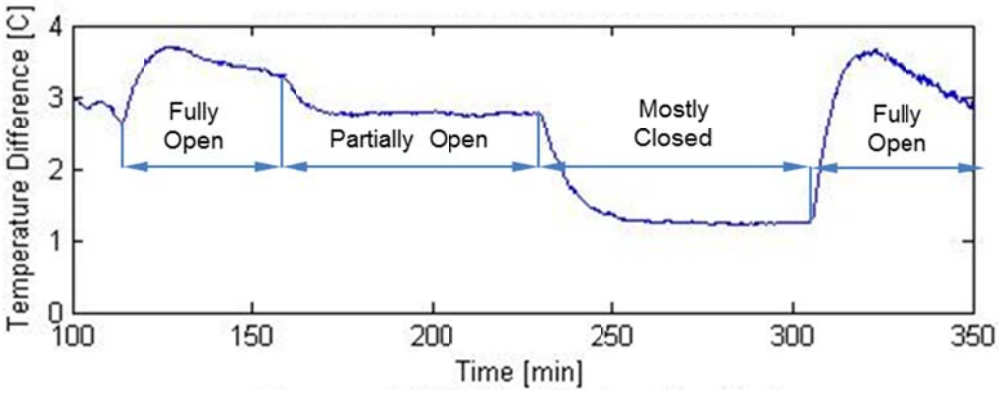

Figure 20. Temperature difference across evaporator (1/8/14).

D. Water Absorption Capacity and Final LiCl Concentration

The LCAR panels were uncoupled from the system and weighed before and after each absorption and regeneration run to measure the changes in water content. Figure 21 shows results throughout the test series. The amount of water absorbed or desorbed varies from test to test, primarily because the criterion for stopping depends on measured temperatures which vary across each panel and depend on specific test conditions. The maximum water change measured in either a regeneration or absorption test is the best indicator of the water absorption capacity of the LCAR. From the data in Figure 21, we can conclude that the LCAR water absorption capacity is approximately 240 g, corresponding to an energy absorption capacity of 167 W-hr.

Based on the water capacity measurements, we believe that final LiCl concentrations in the range 43 to 45% are possible. Figure 22 plots the final concentration as a function of water absorbed for three different values of initial concentration. Note that final concentrations are quite insensitive to the starting concentration, since the amount of water contained in the solution at the start of an absorption run is much smaller than the amount of water at the end. For an absorption capacity of 240 g water and the LiCl loading of 213 g per panel, the final LiCl concentration will be 43 to 45%.

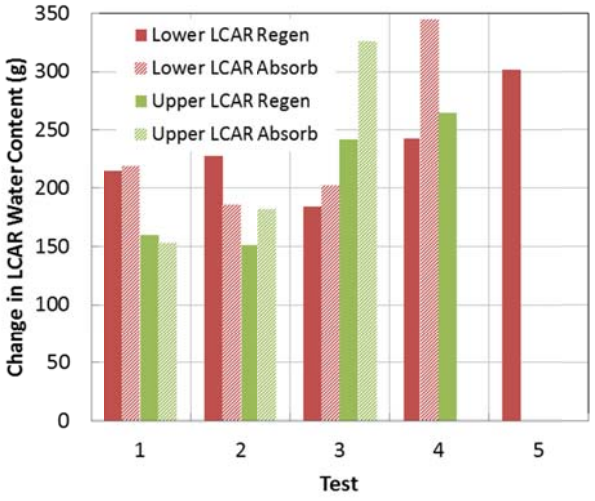

Figure 21. Changes in LCAR water mass during test series.

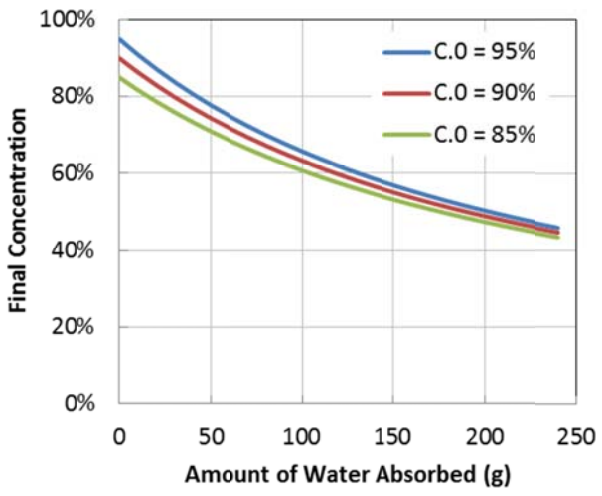

Figure 22. Final LiCl concentration is insensitive to initial concentration.

V. Scaling to Space Suit Conditions

We assessed critical aspects of the SEAR technology and its potential for use in future exploration space suits. Key elements of this assessment were:

- Scaling the LCAR cooling capacity (W-hr) to future space suits with advanced honeycomb designs. We believe that 250 W-hr/ft² should be possible.
- Scaling the LCAR cooling rate (W) to future space suits where the LCAR doubles as the PLSS housing. We believe that heat rejection rates in the range 150 to 300 W should be possible, depending on the LCAR and environmental temperatures.
- Comparing the SEAR to competing thermal control technologies.

E. Scaling LCAR Cooling Capacity

The cooling capacity of the LCAR is expressed in units of W-hr/ft², and is equivalent to the LCAR's ability to absorb water. We scaled the current LCAR cooling capacity to future LCAR designs, assuming that future units would incorporate improved internal structures that approach a true honeycomb geometry and allow more space for the LiCl absorber elements. The baseline cooling capacity of the current LCAR design can be estimated in two ways: (1) based on amount of LiCl that the LCAR can hold, and (2) based on the W-hr of heat rejection measured in thermal vacuum tests.

It is straightforward to estimate the amount of LiCl that can be held in future LCAR designs. The 1 ft² panels tested in this project were charged with 213 g of LiCl. Potential future improvements in LiCl capacity can be estimated based on the measured pressure retention capability of the current design. The pressure retention capability of the current LCAR has been measured to be about four times greater than actually needed. Therefore, a future unit built using similar fabrication methods could increase the amount of internal volume available for LiCl by reducing the internal area used to support internal pressure loads. This would be accomplished by increasing the size of the pockets in the absorber layer (Figures 6 and 7) that contain the absorber sponges. If the thickness of the future LCAR is still limited to 0.5 in., then the possible improvement in LiCl charge can be computed by reducing the area occupied by structural elements by a factor of four. Table 5 shows the result of this scaling calculation. Also shown is the best possible storage density in a "true" honeycomb structure (like the one shown in Figure 5), in which nearly the entire internal volume can be used for LiCl storage. We believe that it should be feasible to construct this type of structure, although it will require development of improved fabrication methods.

Table 5. LiCl storage density.

	Phase III Design (as built)	Phase III Design With Optimized Internal Structure	"Perfect" Honeycomb
LiCl Storage Density (kg LiCl / ft²)	0.213	0.267	0.281
Mass of LCAR Structure (w/o LiCL) (kg/ft^2)	1.37	1.33	1.32
Total Dry Mass (kg/ft^2)	1.58	1.60	1.60

The cooling capacity can be computed based on the amount of water that can be absorbed in the LiCl solution. The water absorption capacity depends on the amount of LiCl in the LCAR and the solution concentrations at the beginning and end of an EVA sortie:

$$m_{w,a} = m_{LiCl}\left(\frac{1}{C_f} - \frac{1}{C_0}\right) \quad (1)$$

Cooling capacity is simply the amount of water that can be absorbed by the LCAR multiplied by the heat of evaporation (h_{fg}), which will equal the cooling provided by the SWME when operating in a SEAR system. Figure 23 plots the cooling potential per square foot of LCAR radiating area calculated using Eq. (1), assuming a LiCl storage density of 267 g/ft² (corresponding to the "optimized internal structure" design in Table 5). The calculation shows that the cooling capacity depends strongly on the final LiCl concentration (C_f), while the dependence on starting concentration (C_i) is relatively weak. The final concentration that can be achieved in the LCAR will be limited by the increase in water vapor pressure at low LiCl concentrations. Figure 24 plots calculated water vapor pressure in equilibrium with LiCl solution as a function of C_f and the final radiating temperature using relations for water vapor

pressure over LiCl solution (Conde 2009). Since the water vapor pressure in the SWME will be 16 to 17 torr, a vapor pressure in the LCAR that exceeds about 15 torr will reduce the cooling rate due to insufficient pressure difference to drive water vapor flow from the SWME to the LCAR. The calculations show that it will be difficult to reduce the final LiCl concentration to less than 45% while maintaining a radiating temperature of 50°C. Referring to Figure 23, this final concentration corresponds to a cooling capacity of about 200 W-hr/ft². Higher capacities are possible if there is enough radiating surface (or an environment that is cold enough) to enable operation at 45°C at the end of a mission.

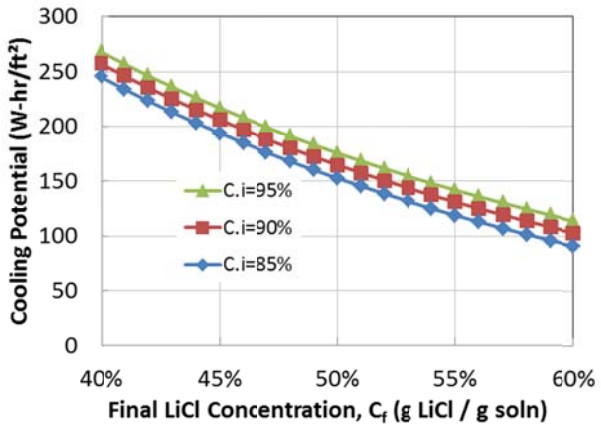

Figure 23. Calculated LCAR cooling capacity depends strongly on LiCl concentrations at beginning and end of sortie (based on 267 g LiCl/ft²).

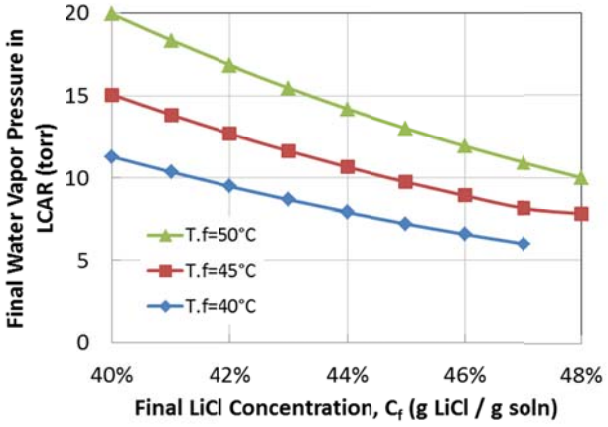

Figure 24. Calculated LCAR final concentration can be limited by vapor pressure over solution.

From this analysis, we conclude that the heat absorbing capacity of the LCAR will be approximately 250 W-hr/ft². This value is possible despite the vapor pressure limitations at the end of a sortie (shown in Figure 24), since the increased vapor pressure of the dilute LiCl solution will simply result in a lower radiator temperature. Although the cooler radiator rejects a reduced amount of heat, it can still absorb part of the water produced by the SWME. Water in excess of the radiating capacity will be vented, the same way that excess water will vent early in a sortie when high metabolic rates exceed the radiating capacity.

The cooling capacity data from tests of a single LCAR panel (Figure 13) can also be used to estimate cooling capacity. These data show a cooling density in the process demonstrator LCAR of 150 W-hr/ft². "True honeycomb" scaling from this level predicts an ultimate cooling capacity of 240 W-hr/ft².

F. Scaling LCAR Cooling Rate

While the total amount of cooling available from the LCAR depends on the amount of LiCl it holds, the instantaneous rate of cooling depends mainly on the surface area available on the PLSS housing and the environmental temperature. Assuming that the LCAR is mounted on the external surfaces of the PLSS backpack, and each panel has a view factor to the environment of 1.0, then the cooling provided by radiation from the LCAR can be computed by:

$$q = A_{LCAR}\,\sigma\,\varepsilon\,(T_{LCAR}^4 - T_{sink}^4)\left(\frac{h_{fg}}{h_{fg}+h_{abs}}\right) \quad (2)$$

The ratio $h_{fg}/(h_{fg}+h_{abs})$ accounts for the fact that the heat generated when water vapor is absorbed in LiCl solution includes both the heat of condensation (h_{fg}) and the heat of absorption (h_{abs}). As a result, the cooling generated in the SWME is less than the radiated heat by this fraction. The emissivity of the Aeroglaze coating used for the LCAR is 0.9. The surface area available on an advanced EMU will be about 7.5 ft² (0.697 m²). Results of the radiation calculation using these values are shown in Figure 25a, assuming an average value for h_{abs}/h_{fg} equal to 0.15. The radiating power of the LCAR is in the range 150 to 300 W, depending on the temperatures of the LCAR and the heat sink.

A second way to compute the cooling power is to divide the cooling capacity (in W-hr) by the duration of an EVA sortie. Results of this calculation are shown in Figure 25b. Comparison of Figure 25a and Figure 25b shows

that the actual rate of heat rejection from the LCAR will almost always be more limited by the quantity of LiCl contained in the panel than by the thermal radiation rate. However, for low values of final LiCl concentration and warm environments, thermal radiation can become a limiting factor.

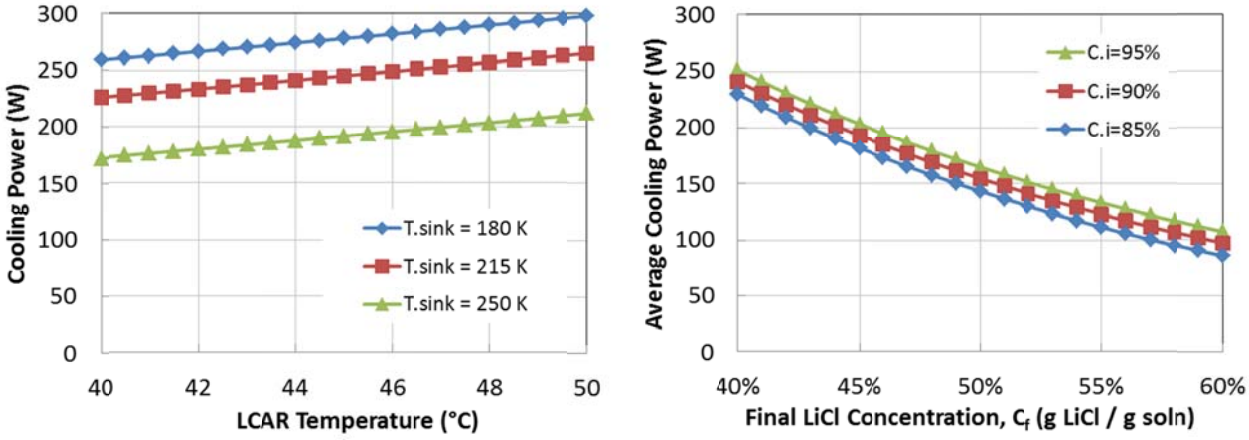

(a) Based on 7.5 ft² LCAR area and radiation temperatures

(b) Based on LiCl loading and sortie duration of 8 hr ($h_{abs}/h_{fg} \approx 0.15$)

Figure 25. Calculated heat rejection rates from the LCAR.

G. Comparison With Competing Thermal Control Technologies

We compared the LCAR with other methods of heat rejection for future EVA suits. We considered several design variants:

- The current EMU design (sublimator only). The calculations assume that an advanced EMU sublimator would no longer need a slurper to remove humidity condensate, which would be removed in the rapid cycle amine system instead. We used a mass of 4.8 lb_m, which is the mass of the present EMU sublimator.
- A future EMU design that uses the SWME only. The Gen 2 SWME has a mass of 4.1 lb_m and a cooling capacity of 800 W. Therefore, 4.1 lb_m was used for this comparison.
- A SEAR system, assuming T_{sink} = 250 K. This system combines the 4.1 lb_m SWME with a 7.5 ft² LCAR.
- A SWME + simple radiator system, with cases for T_{sink} = 180 K and 250 K.

The simple radiator system assessment assumes that a 7.5 ft², very thin (0.5 mm) aluminum panel radiator cools the LCVG circulating fluid before it enters the SWME. Since this radiator does not have the heat pumping feature of the LCAR, it is not capable of rejecting as much heat as the LCAR. Nevertheless, the partial cooling provided by the simple radiator reduces venting by prechilling the water before it enters the SWME. Note that this thin panel is structurally weak, and therefore cannot replace the PLSS housing. This type of radiator panel cannot prevent freezing in cold environments, so would need additional features (and corresponding mass) to be used in an actual space suit PLSS.

Table 6 shows the results of this assessment. The lightest-weight system (13.2 lb_m) uses the SWME alone and vents 9.1 lb_m of water during an 8-hr EVA. Adding the aluminum radiator adds radiator mass but reduces the amount of water discharge, for a net addition of only 1.3 lb_m. However, the simple radiator system still discharges 3.4 to 6.0 lb_m of water for each 8-hr EVA. The SEAR system saves the maximum amount of water even at the highest ambient temperature. However, the on-back mass penalty is greatest for SEAR, with a net addition of 5.1 lb_m compared to the SWME alone. Even more water could be saved (at the expense of greater mass) if additional LiCl could be held in the LCAR. This could be achieved, for example, by increasing its thickness beyond the 0.5 in. currently assumed. For long-duration exploration missions, the SEAR system offers the maximum benefit for overall water conservation. Overall system trade studies will be needed to evaluate the benefits relative to the penalty of additional on-back mass.

Table 6. Heat rejection technology sizing results (based on an 8-hr EVA).					
	Mass of Sublimator Alone (lb_m)	Mass of SWME Alone (lb_m)	SEAR mass (lb_m)	SWME + Simple Radiator (lb_m)	SWME + Simple Radiator (lb_m)
			T_{sink} = 250 K	T_{sink} = 180 K	T_{sink} = 250 K
Evaporator	4.8	4.1	4.1	4.1	4.1
Radiator	0	0	18.1	4.4	4.4
Water Charge	9.1	9.1	9.1	6.0	6.0
Housing Credit	0	0	-13[8]	0	0
On-back Mass	13.9	13.2	18.3	14.5[9]	14.5[9]
Water Discharged	9.1	9.1	3.3	3.4	6.0
Water Saved by the Radiator			5.8	5.7	3.1

VI. Conclusions and Forward Work

This work has demonstrated the feasibility of building a flat panel LCAR for use in a SEAR system with improved thermal performance compared to earlier prototypes. The conclusions from this work are as follows:

- It is feasible to build LCAR panels that have a thin, planar configuration, high volumetric packing density for LiCl, and high internal mass transfer area.
- The honeycomb LCARs are structurally sound and retain their integrity across the range of expected operating conditions.
- Aeroglaze coatings provide a high-emissivity (0.90) radiating surface for the LCAR panels.
- The honeycomb LCARs provide a highly uniform radiating temperature (±10°F) across their entire surface.
- The honeycomb LCARs operate well with vapor produced by a SWME, showing the feasibility of operating a SEAR system.
- The internal gas flow design and high thermal conductivity of the honeycomb LCAR prevent direct condensation and freezing of water vapor during operation.
- The honeycomb LCARs are capable of up to 250 W-hr/ft² total heat rejection.
- The honeycomb LCARs are capable of radiating powers up to 45 W/ft². Higher radiating powers are possible early in a mission, when the LiCl concentration is higher. Radiating power gradually decreases as the LiCl concentration decreases.
- The SEAR system can save much more water in a wider range of environments than competing heat rejection systems.

Based on these findings, we identified the next steps for continued development of the SEAR technology incorporating multifunctional LCAR units. These next steps would involve:

- Continued development of fabrication methods with the goal of boosting the LiCl capacity of the LCAR panels by moving towards a true honeycomb structure.
- Structural, shock, impact, and vibration tests of assembled LCAR panels to validate fabrication and design methods.
- A full safety analysis of the LCAR to confirm that LiCl containment and immobilization are adequate for flight operations.
- Development of detailed analysis methods for the absorption and regeneration processes in the LCAR that will enable optimization of future designs.
- Additional testing of the SEAR system with a current-generation SWME to enable optimization of the noncondensible gas venting process.

[8] Based on 7.5 ft^2 of Al panel, 1/8-in. thick.
[9] Does not account for additional mass needed to prevent freezing.

- Design and operational analysis of tests that couple a SEAR system with an EMU PLSS on the ground and on the ISS.
- Development of design concepts and trade-off studies for life support systems on future space suits that incorporate SEAR systems with multifunctional LCAR panels.

Acknowledgments

The authors gratefully acknowledge the support of the Crew and Thermal Systems Division, NASA Lyndon B. Johnson Space Center.

References

Bue, G., Hodgson, E., Izenson, M., and Chen, W., "Multifunctional Space Evaporator-Absorber-Radiator," 43rd International Conference on Environmental Systems, Vail, CO, July 2013, AIAA-2013-3306.

Bue, G., Trevino, L., Tsioulos, G., Settles, J., Colunga, A., Vogel, M. and Vonau W., "Hollow Fiber Spacesuit Water Membrane Evaporator Development and Testing for Advanced Spacesuits," AIAA-2010-6040, 40th International Conference on Environmental Systems, Barcelona, Spain, July, 2010.

Conde, M, "Aqueous Solutions of Lithium and Calcium Chlorides: Property Formulations for Use in Air Conditioning Equipment Design," <http://www.mrc-eng.com/Downloads/Aqueous%20LiCl&CaCl2%20Solution%20Props.pdf, M. Conde Engineering, 2009.

Izenson, M., Chen, W. and Trevino, L., "Lightweight, Flexible, and Freezable Heat Pump/Radiator for EVA Suits," SAE Paper 08ICES-0312, 2008.

Izenson, M. and Chen, W., et al., "Advanced Design Heat Pump/Radiator for EVA Suits," SAE Paper 2009-01-2406, 2009.